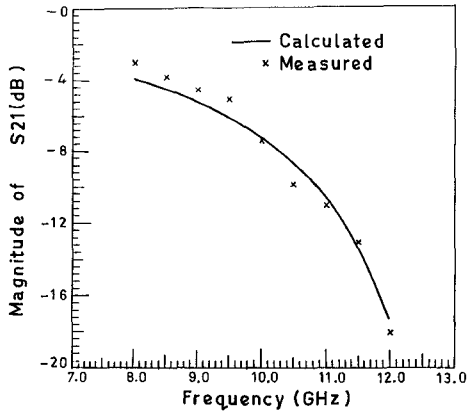

(a)

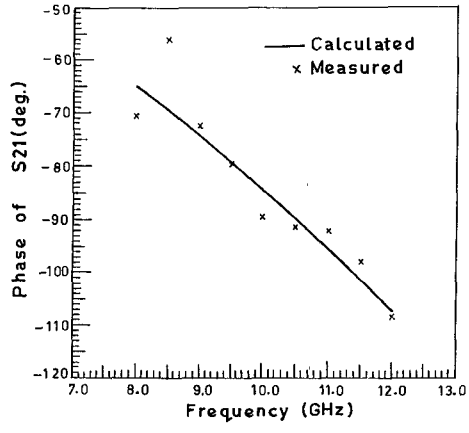

(b)

Fig. 3. Comparison of theoretical and experimental results of (a) magnitude of the transmission coefficient (dB) and (b) phase of the transmission coefficient (degree) $a = 22.86$ mm, $b = 10.16$ mm, $d = 0.7937$ mm, $\epsilon = 2.22$, $h_1 = 10.6363$ mm, $W = 2.032$ mm, $h = 8.16$ mm, $h' = 1.0$ mm, $C = 2.0$ mm.

a comparison of the theoretical and experimental results of $|S_{21}|$ in decibels, and Fig. 3(b) shows the comparison $\angle S_{21}$ in degrees of the sample discontinuity.

V. Conclusion

A new type of discontinuity in the unilateral fin line is analyzed using hybrid mode analysis in conjunction with the Transverse Resonance Technique. Appropriate basis functions are chosen to model the field in the slot and current on the discontinuity strip. Comparison curves of the transmission coefficient for a sample discontinuity are also presented. The two results are shown matching reasonably well, which validates the choice of basis functions.

References

[1] R. Sorrentino and T. Itoh, "Transverse resonance analysis of fin line discontinuity," *IEEE Trans. Microwave Theory Tech.*, vol. MTT-32, pp. 1633–1638, Dec. 1984.

[2] B. Bhat and S. K. Kaul, *Analysis Design and Application of Fin Lines.* Deadham, MA: Artech House, 1987.

[3] T. Itoh, "Spectral domain immittance approach for dispersion characteristics of generalized printed transmission lines," *IEEE Trans. Microwave Theory Tech.*, vol. MTT-28, pp. 733–736, July 1980.

[4] A. K. Gupta, "Characterization of two new types of fin line discontinuities," M.Tech. thesis, A.C.E.S., I.I.T., Kanpur, 1993.

[5] A. Biswas and B. Bhat, "Accurate characterization of an inductive strip in fin line," *IEEE Trans. Microwave Theory Tech.*, vol. 36, pp. 1233–1238, Aug. 1988.

Analysis of Spherical Radar Cross-Section Enhancers

John R. Sanford

***Abstract*—A method for determining the plane wave scattering by a spherical radar cross section enhancer is described. In the two-step process, the desired field representation is expressed as a superposition of vector spherical wave functions. This allows the plane wave scattering from a spherically stratified object to be determined.** *Love's equivalence principle* **is then employed to account for the metallic portions of the spherical reflector. The analysis utilizes the expansions of a plane wave, an electric current element, and a magnetic current element in terms of spherical wave functions. Measured results show fairly good agreement with predicted results.**

I. Introduction

Microwave passive reflectors are widely used to increase the radar cross section (RCS) of target drones or other test vehicles. An extremely effective RCS enhancer is a spherical dielectric lens with an angular sector covered by a conducting surface "cap." Such RCS augmenting devices are produced by a number of firms in Europe and the United States. The principle of the structure is as follows: The spherical lens has a permittivity that varies with radius. We choose a variation that causes the lens to focus a plane wave to a small area on the surface of the lens [1]. The cap reflects this energy back through the lens where it emerges as a plane wave, as depicted in Fig. 1. This combination of lens and cap serves as a passive reflector of microwave energy throughout a solid angle roughly equal to that subtended by the cap.

Here, we outline a method for determining the plane wave scattering by such reflectors. It is a two-step process. First, the desired field representation is expressed as a superposition of mode functions that are chosen in order to permit simple evaluation of the associated boundary conditions. This allows the plane wave scattering from the "capless" lens to be determined on the surface of the device. Afterwards, field equivalence is employed to determine the scattered field of the passive reflector. The analysis requires the expansion of a plane wave, an electric current element, and a magnetic current element in terms of spherical wave functions. The currents on the conductor are assumed to be those dictated by *the equivalence principle.*

II. Spherical Wave Function Expansions

In spherical coordinates, arbitrary fields are represented by a sum of vector spherical wave functions $\boldsymbol{m}$ and $\boldsymbol{n}$ as given by Stratton [2]

$$\boldsymbol{m}_{\substack{e \\ o}mn} = \mp \frac{m}{\sin\theta} Z_n(kr) P_n^m(\cos\theta) \begin{matrix}\sin \\ \cos\end{matrix} (m\phi)\hat{\theta}$$

Manuscript received February 18, 1994; revised September 29, 1994.

The author is with the Department of Microwave Technology, Chalmers University of Technology, 41296 Gothenburg, Sweden.

IEEE Log Number 9410698.

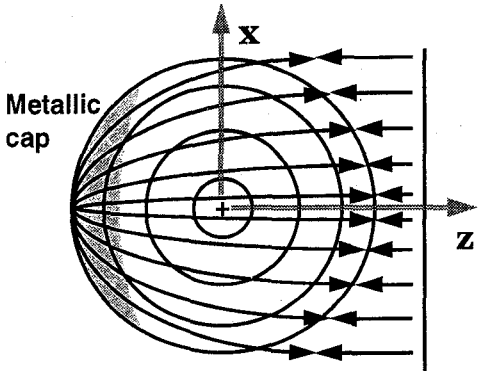

Fig. 1. Spherical RCS enhancer and coordinate axis.

$$- Z_n(kr)\frac{\partial}{\partial\theta}P_n^m(\cos\theta)\begin{matrix}\cos\\ \sin\end{matrix}(m\phi)\hat{\theta} \tag{1}$$

$$\boldsymbol{n}_{\substack{e\\ o}mn} = \frac{n(n+1)}{kr}Z_n(kr)P_n^m(\cos\theta)\begin{matrix}\cos\\ \sin\end{matrix}(m\phi)\hat{r} + \frac{1}{kr}\frac{\partial}{\partial kr}[krZ_n(kr)]\frac{\partial}{\partial\theta} \cdot P_n^m(\cos\theta)\begin{matrix}\cos\\ \sin\end{matrix}(m\phi)\hat{\theta} \mp \frac{m}{kr\sin\theta}\frac{\partial}{\partial kr}[krZ_n(kr)] \cdot P_n^m(\cos\theta)\begin{matrix}\sin\\ \cos\end{matrix}(m\phi)\hat{\phi} \tag{2}$$

where $\hat{r}$, $\hat{\theta}$, and $\hat{\phi}$ are unit vectors in the coordinate directions. The use of e or o denotes the even nature of the cosine function and the odd nature of the sine function. The spherical Bessel function of arbitrary type is represented by $Z_n(kr)$. The type is determined by the field region of interest [3]. A general solution of the vector wave equation requires a linear combination of the even and odd components of both $\boldsymbol{m}$ and $\boldsymbol{n}$ for all orders m and n. The coefficients can be determined since the $\boldsymbol{m}$'s and $\boldsymbol{n}$'s form an orthonormal basis for the vector space of solutions. The expansions of sources with a number of symmetries simplifies the undertaking by imposing criteria forcing some of the coefficients to zero [3]. When we prescribe that the incident field has an x-oriented polarization and is symmetric about the y-axis, we find that the fields are represented by

$$\boldsymbol{E} = E_0\sum_{n=1}^{\infty} i^n\frac{2n+1}{n(n+1)}[a_n\boldsymbol{m}_{o1n}^{(1)} - ib_n\boldsymbol{n}_{e1n}^{(1)}] \tag{3}$$

$$\boldsymbol{H} = -\frac{kE_0}{\mu\omega}\sum_{n=1}^{\infty} i^n\frac{2n+1}{n(n+1)}[b_n\boldsymbol{m}_{e1n}^{(1)} + ia_n\boldsymbol{n}_{o1n}^{(1)}] \tag{4}$$

where the superscripts indicate the use of the spherical Bessel function of the first kind, $j_n(kr)$, which dictates finiteness at the origin. In exterior regions, the spherical Bessel function of the third kind is required.

This form is particularly useful when considering a x-oriented plane wave traveling in the z-direction. The form of the solution in (3) and (4) is compared to the known representation of a plane wave in spherical coordinates for each vector coefficient [4]. This yields the plane wave coefficients of the vector spherical wave functions explicitly ($a_n = 1$, $b_n = 1$). However, if we have an electric current element, the expansion is found by comparing the known far-field of the current element to the vector spherical wave function [3], which yields the coefficients for the region interior to z'

$$a_n = -\frac{j_n^{(1)}(kz')}{i^n},$$

$$b_n = \frac{(n+1)j_{n-1}^{(1)}(kz') - nj_{n+1}^{(1)}(kz')}{i^{(n+1)}(2n+1)}. \tag{5}$$

The modal expansion technique, as given by Harrington [4, pp. 292], was extended to multiple-layered spherical objects with losses [3], [5]. The approach is summarized below. The total electromagnetic field exterior to the lens is the sum of the source radiation, and the scattered radiation and is represented by

$$\boldsymbol{E} = E_0\sum_{n=1}^{\infty} i^n\frac{2n+1}{n(n+1)} \cdot [a_n\boldsymbol{m}_{o1n}^{(1)} - ib_n\boldsymbol{n}_{e1n}^{(1)} + \alpha_n\boldsymbol{m}_{o1n}^{(3)} - i\beta_n\boldsymbol{n}_{e1n}^{(3)}] \tag{6}$$

$$\boldsymbol{H} = -\frac{k}{\mu\omega}E_0\sum_{n=1}^{\infty} i^n\frac{2n+1}{n(n+1)} \cdot [b_n\boldsymbol{m}_{e1n}^{(1)} + ia_n\boldsymbol{n}_{o1n}^{(1)} + \beta_n\boldsymbol{m}_{e1n}^{(3)} + i\alpha_n\boldsymbol{n}_{o1n}^{(3)}] \tag{7}$$

where the a_n and b_n are the source coefficients given in (5), and α_n^1 are β_n^1 are the scattering coefficients, which have not yet been determined. Each shell of the lossy multiple layered sphere is characterized by a permittivity, permeability, and conductivity. These give rise to boundary conditions between the different spherical shells. When these boundary conditions are applied to shell p, one finds that the transformation of the incident field to the next adjacent shell is represented by a 2×2 matrix and takes the form

$$\begin{bmatrix}a_n^{p-1}\\ \alpha_n^{p-1}\end{bmatrix} = U_n\begin{bmatrix}a_n^p\\ \alpha_n^p\end{bmatrix}\begin{bmatrix}b_n^{p-1}\\ \beta_n^{p-1}\end{bmatrix} = V_n\begin{bmatrix}b_n^p\\ \beta_n^p\end{bmatrix} \tag{8}$$

where U_n and V_n are complex 2×2 matrices whose entries are expressions involving nth order spherical Bessel functions and their derivatives. Equating the tangential electric and magnetic fields on each side of the spherical boundary gives the values for these matrix elements

$$U_n^{p+1} = \frac{1}{\Delta_n}\begin{bmatrix}\zeta_n j_n' - \tau h_n\eta_n' & \zeta_n h_n' - \tau h_n\zeta'\\ \tau j_n\eta_n' - \eta_n j_n' & \tau j_n\zeta_n' - \eta_n h_n'\end{bmatrix} \tag{9}$$

$$V_n^{p+1} = \frac{1}{\Delta_n}\begin{bmatrix}\tau\zeta_n j_n' - h_n\eta_n' & \tau\zeta_n h_n' - h_n\zeta_n'\\ j_n\eta_n' - \tau\eta_n j_n' & j_n\zeta_n' - \tau\eta_n h_n'\end{bmatrix} \tag{10}$$

where the lack of a prime denotes the use of the wave number in the present layer, while a prime uses the materials wave number of the next inner shell ($\rho = kr_p, \rho' = k'r_{p+1}$), and where

$$j_n = j_n(\rho) \qquad h_n = h_n^{(1)}(\rho) \tag{11}$$

$$\zeta_n = \frac{1}{\rho}\frac{\partial}{\partial\rho}[\rho h_n^{(1)}(\rho)] \qquad \eta_n = \frac{1}{\rho}\frac{\partial}{\partial\rho}[\rho j_n(\rho)] \tag{12}$$

$$\Delta_n = j_n\zeta_n - h_n\eta_n \qquad \tau = \frac{k'}{k}\frac{\mu}{\mu'}. \tag{13}$$

Since we are concerned only with the fields in the regions exterior to the sphere, the scattering matrices of each shell are cascaded to obtain

$$\begin{bmatrix}a_n^1\\ \alpha_n^1\end{bmatrix} = S_n\begin{bmatrix}a_n^N\\ \alpha_n^N\end{bmatrix}, \qquad \begin{bmatrix}b_n^1\\ \beta_n^1\end{bmatrix} = T_n\begin{bmatrix}b_n^N\\ \beta_n^N\end{bmatrix} \tag{14}$$

where

$$S_n = U_n^2U_n^3\cdots U_n^N, \qquad T_n = V_n^2V_n^3\cdots V_n^N. \tag{15}$$

The α_n^1, a_n^N, β_n^1, and b_n^N have special significance since they are given by the conditions of finiteness for the fields at the origin and by the incident wave, respectively. Hence, we can now obtain α_n^N and β_n^1 from (14) by a simplified matrix inversion. For far-field computation, we must use the asymptotic form of the Hankel function. The solution technique is independent of the source type, thus our method is valid for any source for which we can determine the spherical wave expansion. As will be shown, computation of the scattering by a

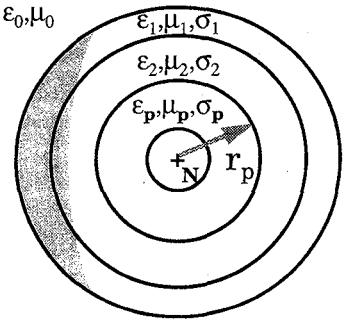

Actual		Optimum Design	
Radius (m)	ε_r (-)	Radius (m)	ε_r (-)
.03755	1.93+.0003j	.0459	1.98+0j
.0552	1.74+.0003j	.0649	1.88+0j
.0741	1.71+.0003j	.0795	1.79+0j
.0838	1.65+.0003j	.0918	1.71+0j
.09415	1.64+.0003j	.1026	1.63+0j
.0994	1.56+.0003j	.1124	1.54+0j
.1184	1.54+.0003j	.1214	1.46+0j
.125	1.50+.0003j	.1298	1.38+0j
.134	1.40+.0003j	.1377	1.29+0j
.1427	1.28+.0003j	.1451	1.21+0j
.1515	1.20+.0003j	.1522	1.13+0j
.1590	1.10+.0003j	.1590	1.04+0j
μ_p=1.0	σ_p=0.0	μ_p=1.0	σ_p=0.0

Fig. 2. Test device electrical parameters.

spherical passive reflector requires both the plane wave coefficients and the current element coefficients given in (5).

Although some assumptions have been made about the orientation of the source, the utilization of a vector coordinate rotation $R(\theta, \phi)$ allows the consideration of any alignment of a radially transverse source [8]. The product of scattering solution of an infinitesimal electric current element and the spherical rotation operator $R(\theta, \phi)$ can be considered the general electric current Green's functions $G^e(\boldsymbol{r}, \boldsymbol{r}')$ for the spherical lens, where $\boldsymbol{r}'$ is the position of the current element, and $\boldsymbol{r}$ is the observation point. Similarly, a magnetic current element Green's function, $G^m(\boldsymbol{r}, \boldsymbol{r}')$ is found by duality. This representation will prove useful in the next section.

III. Reflective Cap

In the previous section, the scattering of spherically stratified geometries is addressed. Plane wave and electric current element excitations are considered. The scattering by an arbitrary current distribution is represented

$$\boldsymbol{E}(\boldsymbol{r}) = \oint [G^e(\boldsymbol{r}, \boldsymbol{r}')\boldsymbol{J}_s(\boldsymbol{r}') + G^m(\boldsymbol{r}, \boldsymbol{r}')\boldsymbol{M}_s(\boldsymbol{r}')]\, dS' \qquad (16)$$

where electric and magnetic currents $\boldsymbol{J}(\boldsymbol{r}'), \boldsymbol{M}(\boldsymbol{r}')$ are unknown. In the following paragraphs, the principles for the characterization of a smooth conductor in the vicinity of a spherical scatterer are discussed. They are then applied to the metallic cap covered lens.

If the fields due to plane wave incidence on a spherical lens are calculated in the region of the lens, equivalence can be applied in order to approximate the currents on any metallic regions. Physical optics principles define a method of replacing a conducting surface by an equivalent current representation. Physical optics is based on *the equivalence principle* and *image theory*. Instead of physical optics, we apply *Love's Equivalence*, which employs both electric and magnetic currents. This formulation is more credible than a single current type formulation since the electric and magnetic fields are not coupled in a trivial way, as with plane wave incidence upon a conducting plane [6, pp. 329–346]. Direct application of *Love's Equivalence* guarantees that the incident fields do not penetrate the metallic cap. The integration of a tangential field on the spherical surface is equivalent to the integration of a surface current density over the same surface. On the metal cap, the induced currents are assumed to be

$$\begin{aligned} \boldsymbol{J}_s &= \boldsymbol{n} \times \boldsymbol{H} \\ \boldsymbol{M}_s &= \boldsymbol{n} \times \boldsymbol{E} \end{aligned} \qquad (17)$$

and everywhere else they are taken as zero. The validity of these approximations is discussed in numerous texts [4], [6], [7]. This gives a method of determining the scattering by an arbitrary conductor in the vicinity of a spherical lens.

The spherical passive reflector is a subset of this problem. The cap is positioned at a fixed radius. Hence, the scattered field need only be computed for a single current element. All other Green's functions are determined by applying the rotation matrix to this scattered field. The computer implementation of the algorithm requires that the integral representation in (16) be represented as a summation. The metallic cap is broken into small, approximately equal area sectors defined by θ, ϕ. Each sector contains the currents dictated by (17). The observation points are assumed to be on a sphere of constant radius that may, but need not be in the far-field of the lens. Consequently, the current element scattering need only be calculated once. The problem has been reduced to one of coordinate rotations and interpolation. The symmetries about the $x = 0$ and $y = 0$ planes reduce the data storage by a factor of 4. Knowledge of the observation region can further decrease the storage requirements. Each Green's function is determined by applying the rotation operator to the stored data. To obtain data at the observation point, a third order B-spline is used to interpolate the Green's function. Methods for the numerical evaluation of the required functions are available [3]. The algorithm has good convergence characteristics for the described geometry.

IV. Results

RCS measurements and calculations were made in order to compare the reflectivity of the spherical lens reflector to the maximum of a flat smooth metallic plate of the same projected area. The parameters of the test RCS enhancer are given in Fig. 2. Fig. 3 shows a prediction of such a reflectivity, which has been generated by the algorithm described above. The results compare surprisingly well with the measured values in the regions of interest. The approximations used for the induced surface currents are valid when the transverse dimensions of the reflector and the radii of curvature of the reflector are much greater than a wavelength. The tested case has roughly a 5.3 wavelength radius of curvature. The good agreement is due in part to the focusing property of the lens, which reduces the edge diffraction of the cap.

The RCS is not more than 5 dB below the theoretical maximum over a 50° opening angle. The design can be improved using a different radii and permittivity profile. The theoretical result of an optimized design is also shown. This displays the two major advantages of the spherical lens reflector over the triple bounce corner reflector: 1) The theoretical cross-section is above that of a circular corner reflector of the same diameter, and 2) The solid angular coverage of the lens is far superior to that of the corner reflector.

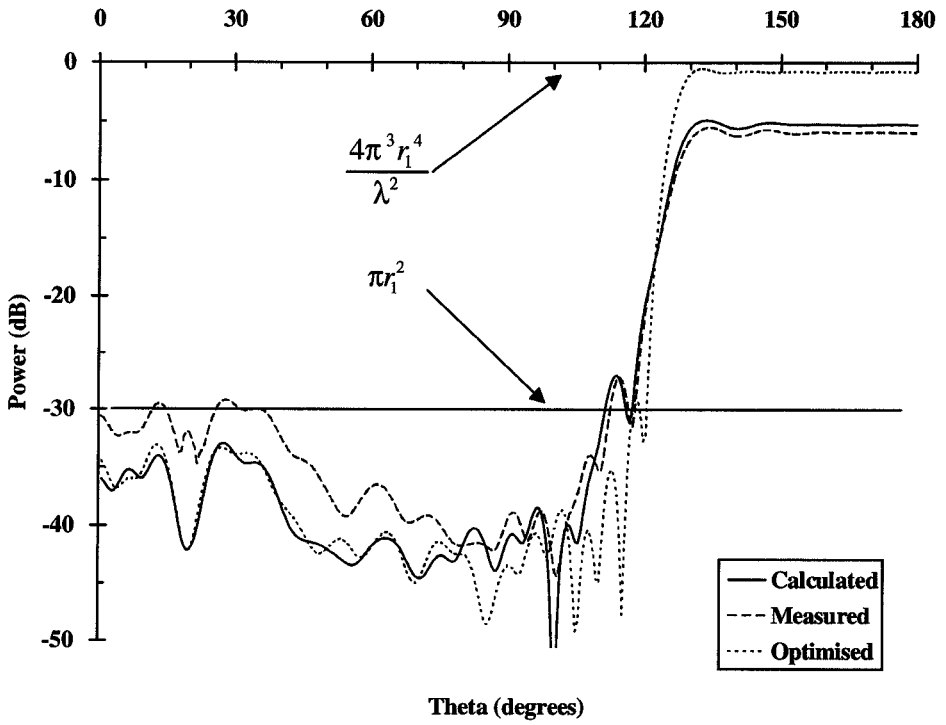

Fig. 3. Reflectivity pattern of a 30-cm diameter passive reflector measured at 10 GHz.

The major disadvantages of the lens geometry are the considerably greater weight and cost.

On a 33-MHz 486PC, the 10-wavelength diameter lens with a cap divided into 2048 sectors requires 40 minutes for the 180-point plot shown in Fig. 3.

V. Conclusion

The method presented here allows the calculation of the scattered fields by a spherical RCS enhancer reflector. The method is highly efficient, and its accuracy is limited only to the validity of equivalent current approximations. The results compare reasonably well with experimental data and demonstrate the usefulness of the device. The physical optics approximation could be replaced by a moment method routine to yield better accuracy.

References

[1] R. K. Luneberg, *Mathematical Theory of Optics.* Providence, RI: Brown University Press, 1944.

[2] J. A. Stratton, *Electromagnetic Theory.* New York: McGraw Hill, 1941.

[3] J. R. Sanford, "Analysis of spherically stratified microwave lens," *Trans. Antennas Propagat.,* pp. 690–698, 1994..

[4] R. F. Harrington, *Time Harmonic Electromagnetic Fields.* New York: McGraw Hill, 1961.

[5] J. R. Wait, "Electromagnetic scattering from a radially inhomogeneous sphere," *Appl. Sci. Res.,* section. B, vol. 10, pp. 441–450.

[6] C. A. Balanis, *Advanced Engineering Electromagnetics.* New York: Wiley, 1989.

[7] W. J. Rush and P. D. Potter, *Analysis of Reflector Antennas.* New York: Academic, 1970.

[8] J. J. Tuma, *Engineering Mathematics Handbook.* New York: McGraw Hill, 1987.